HiSST: 2nd International Conference on High-Speed Vehicle Science Technology
11–15 September 2022, Bruges, Belgium

Modification of the bow shock shape and thermal effects with MHD actuator in supersonic low pressure plasma flows

Viviana Lago[1], *Hugo Noubel*[2], *Creange Mélodie*[3], Jaegly Jonathan[4], Prezeau Juliette[5]

Abstract

This experimental work concerns the ability to modify the bow shock of a Soyuz-type model with an MHD actuator in supersonic and low-density plasma flows. A neodynium magnet inserted into the model creates a magnetic shield on the front side of the model. For comparison, an identical model is used to analyse the generic shock wave under similar operating conditions. Visualization and analysis of the shock wave shape was performed using images of the flow field obtained with an iCCD camera. The temperature of the wall model was measured simultaneously with an IR thermal camera. To investigate the influence of the plasma chemical composition, measurements were made in argon and air plasma streams. The results show that the MHD actuator increases the thickening and distance of the shock wave. The wall temperature of the model is therefore also changed. The rate of temperature increase is slower, which leads to lower values for the maximum temperature reached. Nevertheless, differences were observed depending on the nature of the chemical plasma.

Keywords: *Plasma Flow, MHD experiments, Supersonic, Low pressure, Bow shock modification*

[1] *Laboratoire ICARE, CNRS, 1 C Av de la Recherche Scientifique, Orléans, viviana.lago@cnrs-orleans.fr*
[2] *Laboratoire ICARE, CNRS, 1 C Av de la Recherche Scientifique, Orléans, hugo.noubel@cnrs-orleans.fr*
[3] *IPSA,* Bis, 63 Bd de Brandebourg, 94200 Ivry-sur-Seine
[4] *IPSA,* Bis, 63 Bd de Brandebourg, 94200 Ivry-sur-Seine
[5] *IPSA,* Bis, 63 Bd de Brandebourg, 94200 Ivry-sur-Seine

1. Introduction

The growing interest in magnetohydrodynamic (MHD) actuators to modify the ionised flow fields around vehicles during hypersonic flight has motivated a large amount of numerical and experimental research. MHD flow control was suggested for active flow control and active heat shielding in reentry flights in the 1980s. MHD flow control was suggested for active flow control and active heat shielding in reentry flights in the 1950s and 1960s [1, 2, 3]. Magnetic fields applied to a weakly ionised plasma flow around a reentry vehicle will induce electric currents in the shock layer, whose interaction with the magnetic field generates a Lorenz force, decelerating the plasma flow in the shock layer. As a result, this leads to the widening of the shock layer, attenuating the convective heat flux towards the vehicle [4].

Many works have numerically investigated the effects of MHD as active flow control [5, 6, 7, 8, 9, 10, 11]. Bityurin and Bocharov[12,] and Otsu et al [13] independently demonstrated another interesting effect of MHD flow control: the magnetic field could lead to an increase in drag force as a Lorentz force reaction acts on a magnet installed in a vehicle. The experimental study by Kawamura et al [14] successfully demonstrated the drag increasing effect of MHD flow control using an arc-jet wind tunnel. Nevertheless, the physics is very complex and sophisticated models are needed to describe the coupling between hypersonic aerodynamics, the chemistry of ionized molecular gases and electromagnetic forces. In the numerical simulation of the reentry plasma flow, the management of the thermal non-equilibrium state is one of the important issues. Indeed, a numerical study by Farbar et al. [15] suggested that the consideration of the nonequilibrium state between the electronic, translational and vibrational-electronic modes is of key importance for the prediction of the electron number density under the high-density free flow conditions of the study. In the case of MHD flow control, the numerical consideration of the thermal non-equilibrium state is even more important. Indeed, plasma properties such as electrical conductivity and Hall parameter, which depend on the degree of thermochemical nonequilibrium state, directly influence the strength of the MHD interaction [16]. Few works are listed in the literature concerning experimental investigation on flow control by MHD. These works show that magnetic fields are able to modify the flow close to the model, however their effect on the flow properties are very dependent on the magnetic configuration and the geometry of the body [17, 18, 19, 20, 21, 22].

This paper presents an experimental study on the ability of MHD to act as a heat shield. It is carried out in a supersonic flow and at low pressure and high enthalpy with the arc jet generator in the PhEDRA wind tunnel. In previous studies, we have studied several MH/body configurations to observe the effectiveness of MHD control in modifying the flow properties. In particular, two configurations were tested: a flat, sharp plate and a blunt cylinder, as shown in Figure 1 . The effect of the magnetic field can be clearly seen where the stronger magnetic field region appears as a weaker radiation region of the flow.

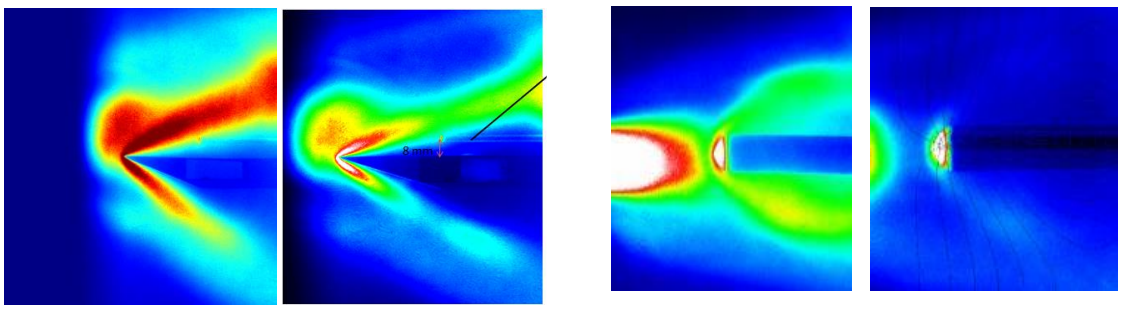

Fig 1. : iCCD images of the flow field obtained in argon plasma around a sharp flat plate and the blunt/cylinder without magnetic field (left) and with magnetic field (rigth)

For both cases, measurements of local pressure, rotational temperature and electron/temperature properties were carried out in the area of the applied magnetic field. It was observed that the magnetic field produces a decrease of 13.7% and 59% respectively of the electron density and an increase of 32% and 38% of the electron density. The electrostatic probe was replaced by a Pitot tube to measure the total pressure in the same location than the electron parameters. Values also showed a decreasing

of the total pressure of 8.4% and 9.5% respectively. The local gas temperature determined from spectroscopy analysis presents a decrease of around 13% while the vibrational temperature increases of 37% in case of air plasma flows [23, 24].

Experimental description

The Phedra facility

Phedra facility, one of the three facilities of the Fast Platform, is devoted to experimentally investigate aerothermodynamic properties of ionized super/hypersonic (Mach 1-8) gas flows at low pressure (1-10 Pa) using an arc-jet as plasma source for a ground-base simulation. The wind tunnel is a cylindrical chamber with a length of 5 meters, a diameter of 1.2 meters and a wall thickness of 8 mm. Aluminium cover at the inside of the steel chamber protects it from corrosion. The wind tunnel is equipped with numerous 300- and 500-mm diameter portholes for the passage of fluids and the installation of diagnostics, particularly optical diagnostics.
A steel tube with 400 mm diameter connects the wind tunnel with the vacuum system presented on Figure 2. The three-stage pumping system MPR consists of three primary pumps working parallel and three parallel high vacuum pumps providing a total capacity of about 26 000 m^3/h.

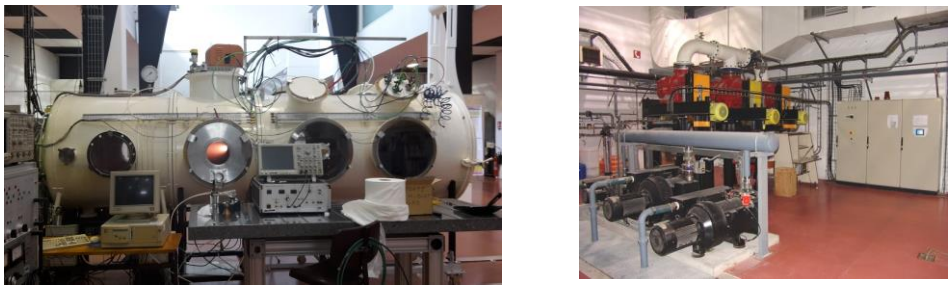

Fig 2. : PHEDRA wind tunnel and pumping group

The plasma source used in the Phedra wind tunnel is an arc-jet type generator. The main design criteria of the generator are satisfactory plasma jet stability, ignition without electrode destruction and easy accessibility for maintenance. The generator consists of a conical nozzle with a cylindrical tungsten throat and a cathode with a zirconium insert, both water-cooled. A stabilised current supply is used to create a stable low-pressure plasma flow.
The plasma generator is mounted on a two-axis linear translation system inside the wind tunnel. Stepper motors allow positioning in vertical and horizontal directions and adjust with precision the position of the model in the plasma flow.

The model description

The model is based on the design of the vehicle that did the most important number of atmospheric re-entry in history: Soyuz. This specific Soyuz, the LOK SA shown on Figure 3, was supposed to bring back cosmonauts on Earth after a Russian mission on the Moon. For this experiment, only the front shape of the vehicle, and in particular the heat shield, is considered. A scale model that can be integrated into the ICARE facilities has therefore been created with a scale factor of 1:67. The test capsule has a diameter of 30 mm and a mass of 22 g. A 22 mm diameter hole has been drilled through the depth of the model to place the system that will create the magnetic field. The CAD design is shown in Figure 4.

Two identical models are used for this experiment. In one, a set of permanent magnets fills the cavity; in the other, the cavity is filled with the same magnets that have been demagnetized. A movable arm that positions them alternately in the plasma flow during the experiments supports the models.

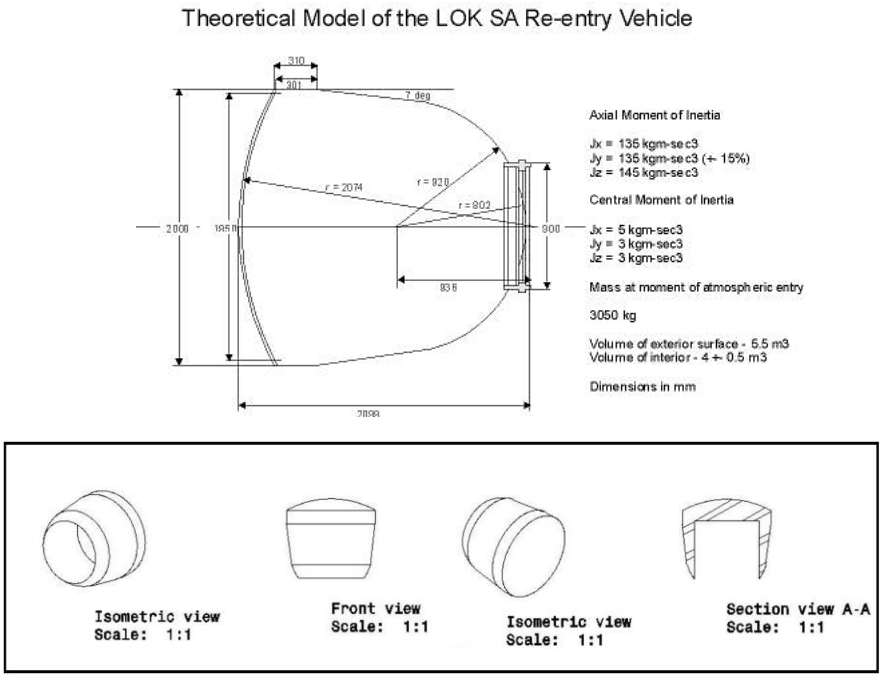

Fig 3. : Design of the Soyuz probe (Credit: © Mark Wade) and the experimental test model

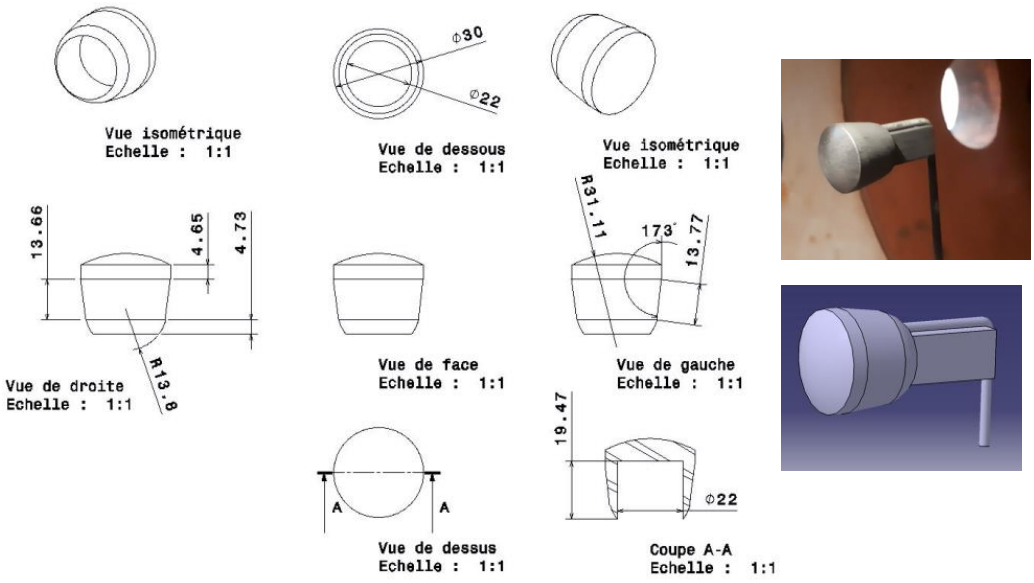

Fig 4. *:* Assembly of capsule, magnet and threaded holding rods

For this experiment, the magnetic field should have a radial orientation to deviate the plasma in the right direction thanks to Lorentz forces. The magnetic field was created with a permanent magnet type NdFeB with a rectangular shape of 50x15x15 mm. Therefore, the magnetic field created around the capsule should have a magnitude between 0.3 and 0.5 tesla. To have an order of magnitude, the magnetic field of Earth is around 0.5 μT. Figure 5 presents the magnetic field configuration calculated with the free software FEMM considering the geometry and the properties of the neodymium magnets included in the Femm library.

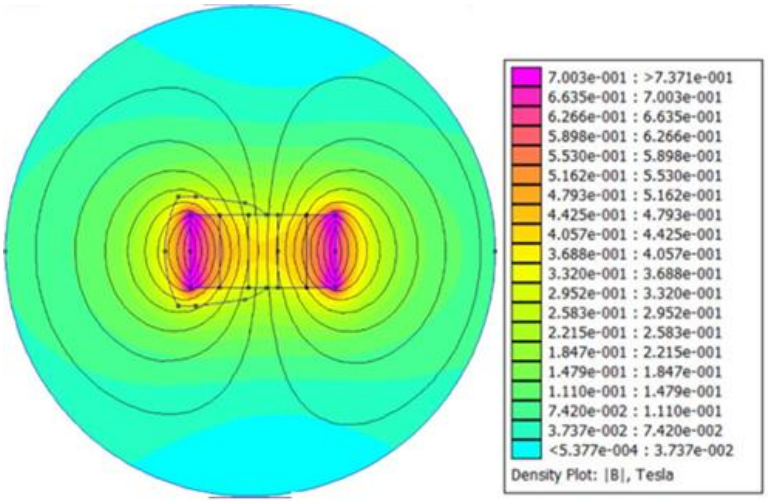

Fig 5. *:* Static calculation of the magnetic field lines of the capsule with a Neodymium magnet N50x15x15 simulated with the software FEMM

Diagnostics and measurement protocol

The objective was to examine whether the presence of a magnetic field could change the shape and distance of the shock and hence the surface temperature of the model. An iCCD 2048 x 2048 Kuro camera placed on the side window aligned with the model was used to visualize the flow around the model. Thermal measurements were carried out with the Infra-red thermal OPTRIS PI 400 camera. The spectral range of the IR camera is between 7.5µm and 13µm. The IR camera was placed on the opposite side of the wind tunnel and focused the entire surface model through a zinc selenium (ZnSe) window, compatible with the IR wavelength range of the camera. For this purpose, the models are coated with a high-temperature black paint.
Both models (magnetized and demagnetized) are mounted on a mechanical piston, as shown in Figure 6. This system allows the choice of putting only one of the two models in the flow, or removing both models from the plasma flow.

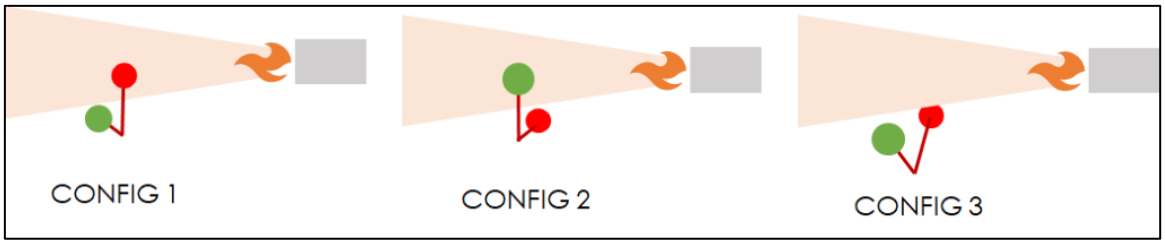

Fig 6. In config 1, only the magnetized capsule is in the flow, in config 2, only the demagnetized capsule is in the flow, and in config 3, both models are out of the flow

To ensure that both cameras would observe exactly the same phenomena, they were adjusted very precisely with a laser beam so that they were at the same height and distance from the models. As the magnetic field is vertically symmetrical, the flow changes observed by the two cameras are identical. This configuration therefore allows the simultaneous collection of thermal and light intensity information on the same event.

2. Results

Experiences have been carried out in Argon and Air plasmas flows. The distance between the exit of the nozzle and the model was of 70 mm. Table 1 presents the operating plasma conditions.

Tab. 1 : Plasma operating conditions

Plasma	**Arc current (A)**	**Arc Voltage (V)**	**Free stream pressure (Pa)**	**Mass Flow rate (g/s)**
Air	100	50	5.3	0.3
Argon	100	30	3.4	0.43

It is important to give the electron density and temperature in order to better assess the effects of the magnetic field. Electrostatic probe measurements have been carried out in the past in free stream plasma for the given operating conditions of Table 1 and are summarized in the Table 2.

Tab. 2 : Electron and density values in free plasma flow

Plasma	**Electron density (cm^{-3})**	**Electron temperature (K)**
Air	2.1 10^{13} (2.5 %)	7980 (1.9%)
Argon	7.3 10 ^{12} (3.5%)	5450 (2.1 %)

Changes in the shape of the shock have been observed, as illustrated in Figure 7 with an Argon plasma flow.

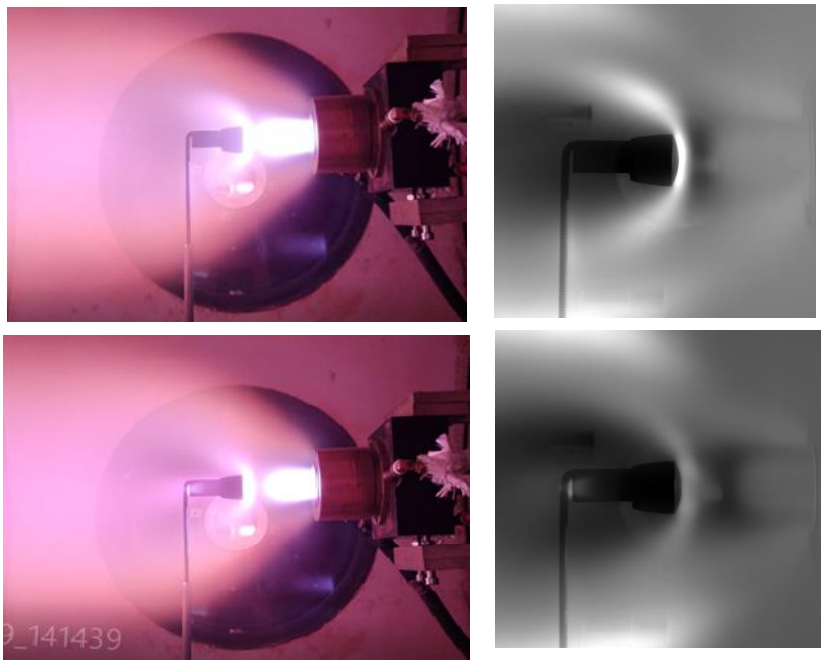

Fig 7. Pictures of the model in Argon plasma Flow, without magnetic field (top) with magnetic field (bottom)

The comparison between the model with and without magnetic fields shows that the shock is thicker and more enveloping around the model in the absence of magnetic fields. The images obtained with the Kuro camera and shown in the figure are the result of post-processing. Each image results from an

average of a series of 50 images obtained with 10 ms of acquisition. The images with the model are corrected by dividing the average image by the average image of the free plasma flow. A measurement set consists of three recordings: a series of images in free flow, a series with the model without magnetic field and a series with the model with the magnet. In this way we are free from possible changes that would be due to a possible fluctuation or drift of the plasma operating conditions.

Figure 8 shows the results of the thermal measurements recorded with the IR camera in an argon plasma flow. On the left, the model has no magnetic field, and the maximum temperature reached on the front of the model was 71.1 C. For the same duration of exposure in the plasma, the model with magnetic fields has a maximum temperature of 53 C.

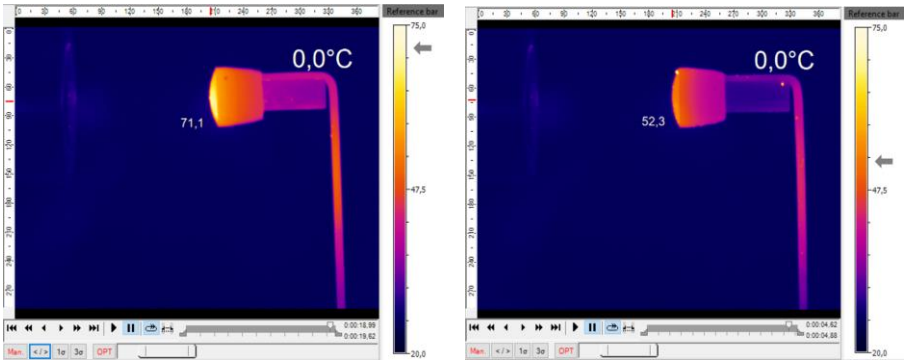

Fig 8. Thermal measurement in Argon plasma. without magnetic field (left) with magnetic field (right)

Figure 8 shows the results of the thermal measurements recorded with the IR camera in an argon plasma flow. Smaller surface temperatures are reached with the model /magnet (picture on the right).

The average temperature of the frontal zone of the model surface is determined from the IR thermal records. Three series of measurements were made under the same argon plasma operating conditions. The measurements are considered from the moment the models are in the plasma flow. The temperature increase experienced by the models for a duration of approximately 3.5 seconds is plotted in Figure 9, for the three series.

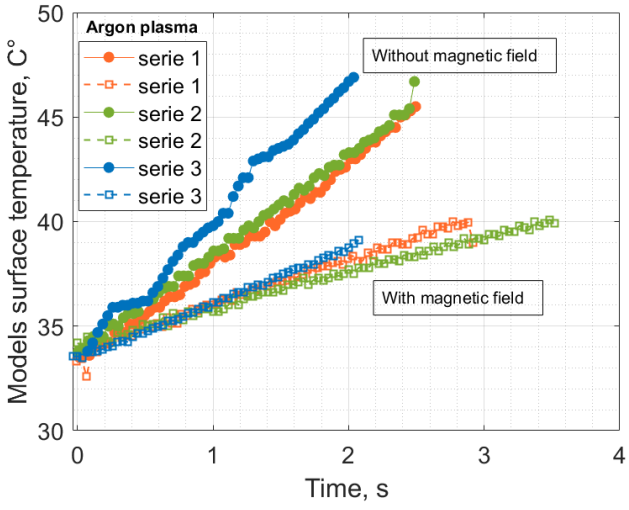

Fig 9. Thermal measurement in Argon plasma. Effects of the magnetic field on the surface temperature of the front surface model

It is observed that the rate of temperature increase is greater for the models without magnetic fields. Considering the three series, the increase rate is 5.4 for the case without MHD and 2.2 for the case with MHD control, i.e. a decrease of 40%.

In terms of flow field modification, the presence of magnetic fields will induce a decrease in the light intensity of the shock even around the model as well as an increase in the distance of the shock from the surface of the model as shown in Figure 10. The shock also appears thicker with the magnetic field acting as a shield. This means that there will be less interaction between the shock and the model wall, which may lead to a decrease in thermal load.

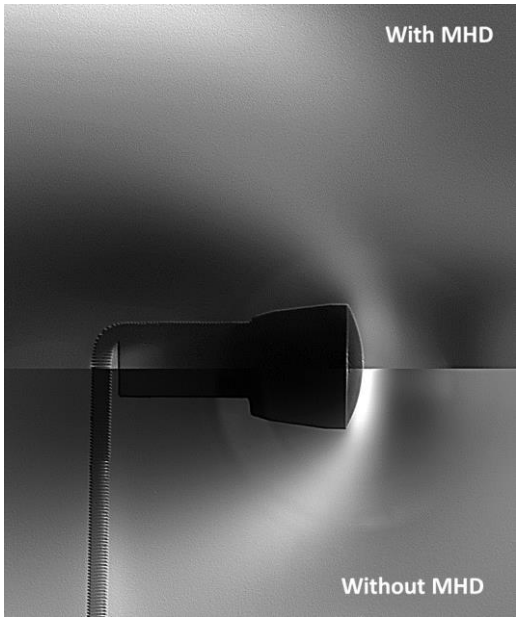

Fig 10. Comparison of the flow field around the model with MHD (top) and without MHD (bottom) in Argon plasma flow

Identical analysis has been carried out with the experiments in air plasma flows. Figure 11 plots the increase of the surface model temperature with the two magnetic configurations. The increase rate is of 8.05 with no magnetic field configuration and 6.5 with the magnetic field configuration, giving an advantage of 18 % with the presence of the magnetic field.

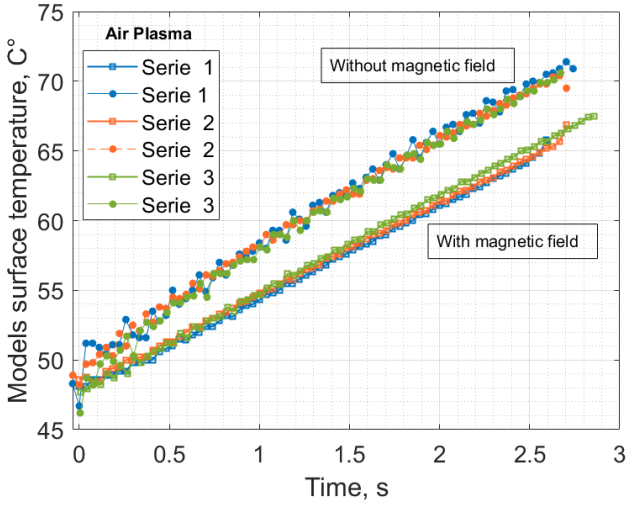

Fig 11. Thermal measurement in Air plasma. Effects of the magnetic field on the surface temperature of the front surface model

In the case of air plasma flows, the influence of the magnetic field was studied separately from the total emission of the excited plasma molecules and the N2+ molecular ions. In this case an interference filter centred on wavelength 313 nm and 10 nm wide at half height was placed in front of the camera lens. The results presented in figure 12 show that on the basis of the total emission, there is a slight influence of the magnetic field on the thickness of the shock created in the model, as in the case of argon. On the other hand, the difference is more important on the distribution of the N2+ ions of which one can observe a clear decrease of the intensity in the shock layer in front of the model. Indeed, the ions are pushed back by the magnetic forces created by the magnet which results in a different response of the shock wave which can lead to the decrease of the surface temperature of the model observed from the thermal measurements.

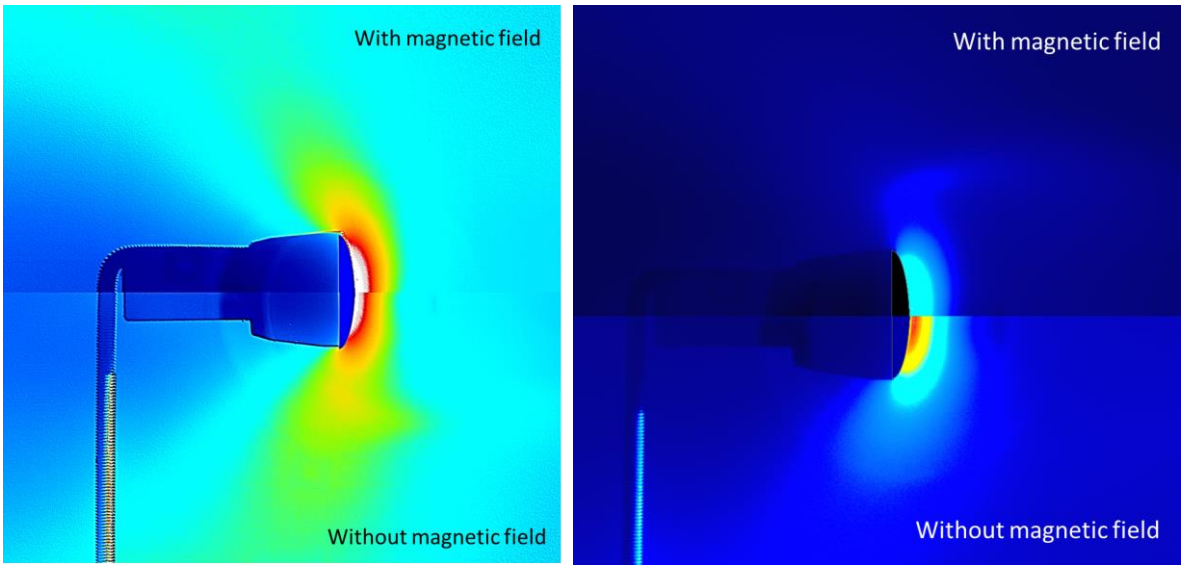

Fig 12. Comparison *of* shock wave modification in Air plasma flow. Without filter (left) and with N_2^+ 391 nm filter (right)

Conclusion

This work looked at the effects that MHD can produce as a heat shield for a probe during atmospheric re-entry. This study is entirely experimental, carried out in the PHEDRA low pressure plasma wind tunnel equipped with an arc jet and producing super and hypersonic high enthalpy flows. The model studied is a reduced model of Souyouz, and the magnetic field was created by a permanent magnet in Neodymium inserted in the model. An identical model without magnetic field was tested in parallel to evaluate the effects of the MHD control. Two types of plasma were studied, a monoatomic Argon plasma and a more complex plasma in thermal disequilibrium of Air. Thermal measurements of the surface of the models were carried out simultaneously with the flow visualisation.
Thermal measurements of the surface of the models were carried out simultaneously with the visualization of the flow. The results show that the magnetic field, in our case oriented radially with respect to the axis of the model, has the effect of modifying the flow especially at the level of the shock layer by reducing the light intensity which results in a decrease in local density. This results in a decrease in the increase in the surface temperature of the model which was confirmed by the thermal measurements which were carried out by thermal camera. The effects are more prominent in the case of argon, as observed in our previous studies with other models geometries and magnetic configurations.

References

1. Meyer, Rudolph C. "On reducing aerodynamic heat-transfer rates by magnetohydrodynamic techniques." *Journal of the Aerospace Sciences* 25.9 (1958): 561-566.

2. Bush, William B. "Magnetohydrodynamic-hypersonic flow past a blunt body." *Journal of the Aerospace Sciences* 25.11 (1958): 685-690.

3. Ziemer, Richard W. "Experimental investigation in magneto-aerodynamics." *ARS Journal* 29.9 (1959): 642-647.

4. Yoshino, Tomoyuki, Takayasu Fujino, and Motoo Ishikawa. "Possibility of thermal protection in Earth re-entry flight by MHD flow control with air-core circular magnet." *IEEJ transactions on electrical and electronic engineering* 4.4 (2009): 510-517.

5. Poggie, Jonathan, and Datta V. Gaitonde. "Magnetic control of flow past a blunt body: Numerical validation and exploration." *Physics of Fluids* 14.5 (2002): 1720-1731.

6. Bityurin, Valentin, and Aleksey Bocharov. "On efficiency of heat flux mitigation by the magnetic field in MHD re-entry flow." *42nd AIAA Plasmadynamics and Lasers Conference in conjunction with the 18th International Conference on MHD Energy Conversion (ICMHD)*. 2011.

7. *Otsu, H., Konigorski, D., and Abe, T., "Influence of Hall Effect on Electrodynamic Heat Shield System for Reentry Vehicles," AIAA Journal, Vol. 48, No. 10, 2010, pp. 2177–2186. doi:10.2514/1.40372*

8. Fujino, Takayasu, et al. "Influences of Electrical Conductivity of Wall on Magnetohydrodynamic Control of Aeroynamic Heating." *Journal of Spacecraft and Rockets* 43.1 (2006): 63-70.

9. Fujino, Takayasu, et al. "Numerical studies of magnetohydrodynamic flow control considering real wall electrical conductivity." *Journal of Spacecraft and Rockets* 44.3 (2007): 625-632.

10. Kim, Minkwan, and Iain D. Boyd. "Effectiveness of a magnetohydrodynamics system for Mars entry." *Journal of Spacecraft and Rockets* 49.6 (2012): 1141-1149.

11. Palmer, Grant. "Magnetic field effects on the computed flow over a Mars return aerobrake." *Journal of Thermophysics and Heat Transfer* 7.2 (1993): 294-301.

12. Bityurin, Valentine, Alexei Bocharov, and John Lineberry. "MHD flow control in hypersonic flight." *AIAA/CIRA 13th International Space Planes and Hypersonics Systems and Technologies Conference*. 2005.

13. Otsu, Hirotaka, et al. "Feasibility study on the flight demonstration for a reentry vehicle with the magnetic flow control system." *37th AIAA Plasmadynamics and Lasers Conference*. 2006.

14. Kawamura, Masaaki, et al. "Experiment on drag enhancement for a blunt body with electrodynamic heat shield." *Journal of Spacecraft and Rockets* 46.6 (2009): 1171-1177.

15. Farbar, Erin, Iain D. Boyd, and Alexandre Martin. "Numerical prediction of hypersonic flowfields including effects of electron translational nonequilibrium." *Journal of Thermophysics and Heat Transfer* 27.4 (2013): 593-606.

16. Imamura, Yusuke, and Takayasu Fujino. "Numerical simulation of magnetohydrodynamic flow control in reentry flight with three-temperature model." *2018 AIAA Aerospace Sciences Meeting*. 2018.

17. Gülhan, Ali, et al. "Experimental verification of heat-flux mitigation by electromagnetic fields in partially-ionized-argon flows." *Journal of Spacecraft and Rockets* 46.2 (2009): 274-283.

18. Cristofolini, Andrea, et al. "Experimental activities on the MHD interaction in a hypersonic air flow around a blunt body." *41st Plasmadynamics and Lasers Conference*. 2010.

19. Deng, Zhengtao, et al. "Data Analysis of Electromagnetic Shockwave Control Experiment for High Mach Number Ionized Flow Applications." *42nd AIAA Plasmadynamics and Lasers Conference in conjunction with the 18th International Conference on MHD Energy Conversion (ICMHD)*. 2011.

20. Cristofolini, Andrea, et al. "MHD Interaction around a blunt body in a hypersonic unseeded air flow: Experimental results and numerical rebuilding." *18th AIAA/3AF International Space Planes and Hypersonic Systems and Technologies Conference*. 2012.

21. Steffens, Lars, et al. "Flow Characterization and MHD Test in High Enthalpy Argon Flows." *8th European Symposium on Aerothermodynamics for Space Vehicles Proceedings*. No. 89144. 2015.

22. Kkn, Anbuselvan, and K. Reddy. "Measurement of heat-flux for magneto-aerodynamic interaction studies in a hypersonic flow." *47th AIAA Plasmadynamics and Lasers Conference*. 2016.

23. Lago Viviana, and Tinon Emanuelle. "Experimental investigation of supersonic plasmas flow fields modification by magnetic fields." *18th AIAA/3AF International Space Planes and Hypersonic Systems and Technologies Conference* (2012).

24. Coumar Sandra, and Lago Viviana. "EHD and MHD actuators: experimental works to enhance spacecraft control and deceleration during atmospheric entries." *14th International Planetary Probe Workshop (IPPW-14)* (2017).